Fluorophore-Labeled *S*-Nitrosothiols

Xinchao Chen,[†] Zhong Wen,[†] Ming Xian,[†] Kun Wang,[†] Niroshan Ramachandran,[‡]
Xiaoping Tang,[†] H. Bernhard Schlegel,[†] Bulent Mutus,[‡] and Peng George Wang*,[†]

*Department of Chemistry, Wayne State University, Detroit, Michigan 48202, and Department of
Chemistry and Biochemistry, University of Windsor, Windsor, Ontario, Canada N9B 3P4*

pwang@chem.wayne.edu

Received April 2, 2001

A series of fluorophore-labeled *S*-nitrosothiols were synthesized, and their fluorescence enhancements upon removal of the nitroso (NO) group were evaluated either by transnitrosation or by photolysis. It was shown that, with a suitable alkyl linker, the fluorescence intensity of dansyl-labeled *S*-nitrosothiols could be enhanced up to 30-fold. The observed fluorescence enhancement was attributed to the intramolecular energy transfer from fluorophore to the SNO moiety. Ab initio density functional theory (DFT) calculations indicated that the "overlap" between the SNO moiety and the dansyl ring is favored because of their stabilizing interaction, which was in turn affected by both the length of the alkyl linker and the rigidity of the sulfonamide unit. In addition, one of the dansyl-labeled *S*-nitrosothiols was used to explore the kinetics of *S*-nitrosothiol/thiol transnitrosation and was evaluated as a fluorescence probe of *S*-nitrosothiol-bound NO transfer in human umbilical vein endothelial cells.

Introduction

In recent years, *S*-nitrosothiols (RSNOs) have received considerable attention because of their potential role in nitric oxide (NO) storage and transfer in a range of physiological processes.[1] A number of *S*-nitroso adducts have indeed been found in vivo[2] and have been associated with physiological functions.[3] For example, RSNOs serve not only as NO "pools"[4] but also as intermediates in the bioactivation of organic nitrates and nitrites[5] and are involved in altering the function and activity of proteins.[6] Chemical understanding of RSNO formation, decomposition, and transport in biological processes is, therefore, of fundamental importance. Analogous to alkyl nitrites (RONOs), RSNOs may react with nitrogen, sulfur, or oxygen nucleophiles to give free thiol and the corresponding transnitrosation product.[7] The transfer of NO between different thiols via transnitrosation (eq 1) is largely

responsible for the activity of RSNO in vivo[8] and has been suggested to be a signaling mechanism for the control of cellular processes by NO.[9]

$$RSNO + R'SH \rightleftharpoons R'SNO + RSH \qquad (1)$$

The kinetics of the process in eq 1 has recently drawn considerable interest.[7,10] In addition, both photolytic homolysis[10d,11] and catalytic decomposition of RSNO in aqueous solution,[7a] as represented in eq 2, directly relate to the generation of NO free radical in vivo.

$$2RSNO \rightarrow RS-SR + 2NO^{\bullet} \qquad (2)$$

This general instability of RSNO should largely be attributed to the low S–NO bond energies, as indicated by our recent study of homolytic/heterolytic bond dissociation energies (BDEs) of the RS–NO bonds.[12]

Recently, Mutus et al.[13] reported that the fluorescence emission of *N*-dansyl-*S*-nitrosohomocysteine was enhanced about 8-fold upon removal of the NO group

---

* Phone: (313) 933-6759. Fax: (313) 577-5831. E-mail: pwang@chem.wayne.edu.
　† Wayne State University.
　‡ University of Windsor.
　(1) (a) Stamler, J. S. In *S–Nitrosothiols and the Bioregulatory Actions of Nitric Oxide through Reactions with Thiol Groups: The Role of Nitric Oxide in Physiology and Pathophysiology*; Koprowski, H., Maeda, H., Eds.; Springer-Verlag: New York, 1993. (b) Butler, A. R.; Rhodes, P. *Anal. Biochem.* **1997**, *249*, 1. (c) Hogg, N. *Free Radical Biol. Med.* **2000**, *28*, 1478.
　(2) (a) Mannick, J. B.; Hausladen, A.; Liu, L.; Hess, D. T.; Zeng, M.; Miao, Q. X.; Kane, L. S.; Gow, A. J.; Stamler, J. S. *Science* **1999**, *284*, 651. (b) Xu, L.; Eu, J. P.; Meissner, G.; Stamler, J. S. *Science* **1998**, *279*, 235. (c) Stamler, J. S.; Jia, L.; Eu, J. P.; McMahon, T. J.; Demchenko, I. T.; Bonaventura, J.; Gernet, K.; Piantadosi, C. A. *Science* **1997**, *276*, 2034. (d) Stamler, J. S.; Jaraki, O.; Osborne, J. A.; Simon, D. I.; Keaney, J.; Vita, J.; Singel, D. J.; Valeri, C. R.; Loscalzo, J. *Proc. Natl. Acad. Sci. U.S.A.* **1992**, *89*, 7674.
　(3) Gaston, B. *Biochim. Biophys. Acta* **1999**, *1411*, 323.
　(4) Stamler, J. S. *Cell* **1994**, *78*, 931.
　(5) Ignarro, L. J.; Lippton, H.; Edwards, J. C.; Baricos, W. H.; Hyman, H. L.; Kadowitz, P. J.; Gruetter, C. A. *J. Pharmacol. Exp. Ther.* **1981**, *218*, 739.
　(6) Broillet, M.-C. *Cell. Mol. Life Sci.* **1999**, *55*, 1036.
　(7) (a) Williams, D. L. H. *Acc. Chem. Res.* **1999**, *32*, 869 and references therein. (b) Munro, A. P.; Williams, D. L. H. *J. Chem. Soc., Perkin Trans. 2* **2000**, 1794.

　(8) Scharfstein, J. S.; Keaney, J. F.; Slivka, A.; Welch, G. N.; Vita, J. A.; Stamler, J. S.; Loscalzo, J. *J. Clin. Invest.* **1994**, *94*, 1432.
　(9) Park, J. W.; Billman, G. E.; Means, G. E. *Biochem. Mol. Biol. Int.* **1993**, *30*, 885.
　(10) (a) Barnett, D. J.; McAninly, J.; Williams, D. L. H. *J. Chem. Soc., Perkin Trans. 2* **1994**, 1131. (b) Meyer, D. J.; Kramer, H.; Ozer, N.; Coles, B.; Ketterer, B. *FEBS Lett.* **1994**, *345*, 177. (c) Barnett, D. J.; Rios, A.; Williams, D. L. H. *J. Chem. Soc., Perkin Trans 2* **1995**, 1279. (d) Singh, R. J.; Hogg, N.; Joseph, J.; Kalyanaraman, B. *J. Biol. Chem.* **1996**, *271*, 18596. (e) Pezacki, J. P.; Pelling, A.; Klugger, R. *J. Am. Chem. Soc.* **2000**, *122*, 10734. (f) Wang, K.; Wen, Z.; Zhang, W.; Xian, M.; Cheng, J.-P.; Wang, G. P. *Bioorg. Med. Chem. Lett.* **2001**, *11*, 433. (g) Rossi, R.; Lusini, L.; Giannerini, F.; Giustarini, D.; Lungarella, G.; Di Simplicio, P. *Anal. Biochem.* **1997**, *254*, 215. (h) Hogg, N. *Anal. Biochem.* **1999**, *272*, 257. (i) Zhang, H.; Means, G. E. *Anal. Biochem.* **1996**, *237*, 141.
　(11) (a) Sexton, D. J.; Muruganandam, A.; McKenney, D. J.; Mutus, B. *Photochem. Photobiol.* **1994**, *59*, 463. (b) Wood, P. D.; Mutus, B.; Redmond, R. W. *Photochem. Photobiol.* **1996**, *64*, 518.
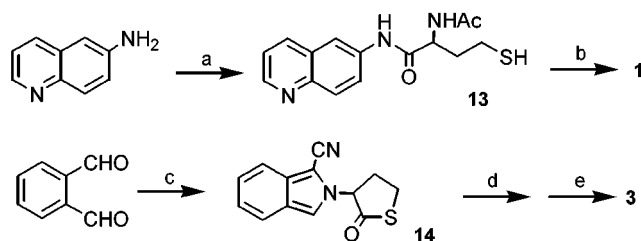　(12) Lü, J.-M.; Wittbrodt, J. M.; Wang, K.; Wen, Z.; Schlegel, H. B.; Wang, P. G.; Cheng, J.-P. *J. Am. Chem. Soc.* **2001**, *123*, 2905.
　(13) Ramachandran, N.; Jacob, S.; Zielinski, B.; Curatola, G.; Mazzanti, L.; Mutus, B. *Biochim. Biophys. Acta* **1999**, *1430*, 149.

Chart 1

1   2   3

4   5   6

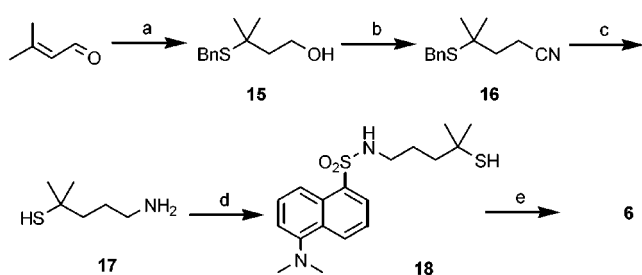7-11 (*n* = 2 - 6)   12

Scheme 1

13

14
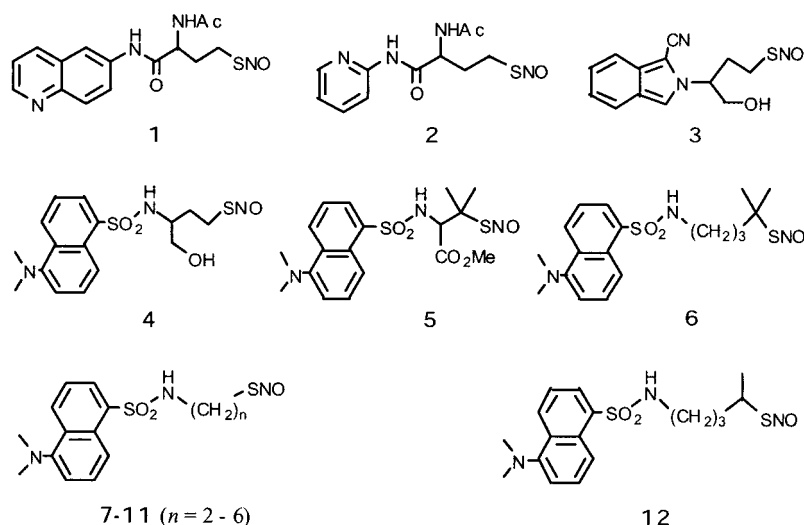
(a) i. 1.0 equiv of NaH, THF, 0 °C, 30 min; ii. *N*-acetyl homocysteine thiolactone, 5 h; (b) *t*-BuONO, MeOH, −20 °C, 2 h; (c) homocysteine thiolactone, NaCN, MeOH/H$_2$O, 4 h; (d) NaBH$_4$, MeOH, 0 °C, 3.5 h; (e) HNO$_2$, −20 °C, 2 h.

Scheme 2

15   16

17   18

(a) i. Benzyl mercaptan, piperidine, reflux, 6 h, 60%; ii, NaBH$_4$, MeOH, 0 °C, 72%; (b) i. BuLi, then TsCl, −78 °C, 1 h, 95%; ii. NaCN, DMF, 90%; (c) i. LiAlH$_4$, THF, reflux, 4 h, 55%; ii. Na, NH$_3$, −40 °C, 70%; (d) Dansyl chloride, DMAP, CH$_2$Cl$_2$, 0 °C, 2 h, 71%; (e) NaNO$_2$/HCl, MeOH/H$_2$O, −20 °C, 92%.

(denitrosation). To explore the mechanism of fluorescence enhancement as well as its potential for detecting thiols (and free cysteines in proteins), we synthesized and evaluated a series of *S*-nitroso compounds (FLSNOs **1**−**12**, Chart 1) linked with different fluorophores. Structural factors relating to the fluorescence enhancements in dansyl-labeled *S*-nitrosothiols (FLSNOs **7**−**12**) were examined using ab initio density functional theory (DFT) calculations. The large fluorescence enhancement for FLSNO **12** was used in the kinetic study of the *S*-nitrosothiol/thiol transnitrosation (eq 1) as well as in the fluorescence microscopic study of RSNO-bound NO transport into the cellular membrane.

Results and Discussion

Synthesis of Fluorophore-Labeled *S*-Nitrosothiols. Twelve *S*-nitrosothiols labeled with a variety of fluorophores including 6-aminoquinoline, 2-aminopyridine, 2-cyanoisoindole, and 5-(dimethylamino)-1-naphthalenesulfonamide (dansyl) were synthesized (Schemes 1−3). Homocysteine thiolactone and its *N*-acetyl derivative were used to introduce the sulfhydryl group in FLSNOs **1**−**3** (Scheme 1).[14] FLSNO **4** was prepared by coupling dansyl chloride with homocysteine thiolactone, followed by reducing the thiolactone with DIBALH. Synthesis of FLSNO **5** started from coupling dansyl

chloride and *S*-trityl penicillamine methyl ester, followed by the routine procedure for deprotecting the sulfhydryl group. The synthesis of tertiary *S*-nitrosothiol **6** is shown in Scheme 2, starting from alcohol **15**, obtained from a two-step procedure reported by Pattenden et al.[15] Scheme 3 shows a general approach for the synthesis of FLSNOs **7**−**11** as well as the synthesis of secondary *S*-nitrosothiol **12**. In the final step of the synthesis of FLSNOs, either *tert*-butyl nitrite (for **1**) or nitrous acid (for **2**−**12**) was used for the *S*-nitrosation reaction. The FLSNO compounds were moderately stable in the PBS buffer (1.0 mM EDTA, 20% MeOH), with half-lives ranging from 3 to 15 h.

Experimental Examination of the Structural Effect on Fluorescence Enhancement through Denitrosation. Both transnitrosation (method A) and photolytic denitrosation (method B) were used to evaluate the synthetic fluorescence probes. In method A, the fluorescence intensities were measured before and after (as A_1 and A_2, respectively) the transformation of FLSNO to fluorophore-labeled thiol using excess glutathione (GSH), and the fluorescence enhancement value was obtained as the ratio of fluorescence intensities (A_2/A_1). Similarly, the fluorescence enhancement value for method B was obtained (as B_2/B_1) via the photolytic denitrosation of FLSNO, which gives rise to disulfides (FL−S−S−FL)

(14) (a) Ramirez, J.; Yu, L. B.; Li, J.; Brauschweiger, P. G.; Wang, P. G. *Bioorg. Med. Chem. Lett.* **1996**, *6*, 2575. (b) Hou, Y.-C.; Wang, J.-Q.; Ramirez, J.; Wang, P. G. *Methods Enzymology Nitric Oxide, Part C: Biological and Antioxidant Activities*; Packer, L., Ed.; Academic Press: 1998, *301*, 242.

(15) Pattenden, G.; Shuker, A. J. *J. Chem. Soc., Perkin Trans 1* **1992**, 1215.

Scheme 3
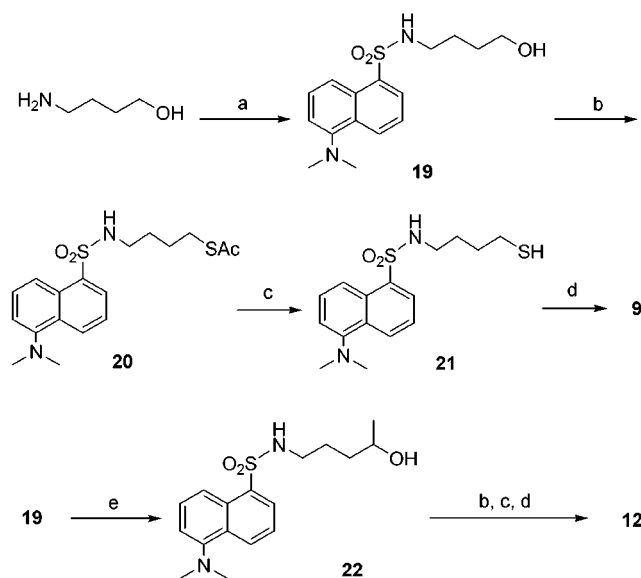
(a) Dansyl chloride, Et₃N, CH₂Cl₂, rt, 83%; (b) i. TsCl, Et₃N, CH₂Cl₂, −20 °C to 0 °C, overnight, 92%; ii. AcSK, acetone, rt, 4 h, 100%; (c) DIBALH, CH₂Cl₂, −78 °C, 2 h, 70%; (d) HCl/NaNO₂, MeOH/H₂O, −20 °C, 2 h, 85%; (e) i. PDC, CH₂Cl₂, rt, 3 h; ii. MeLi, THF, −78 °C, 2.5 h, 60% (two steps).
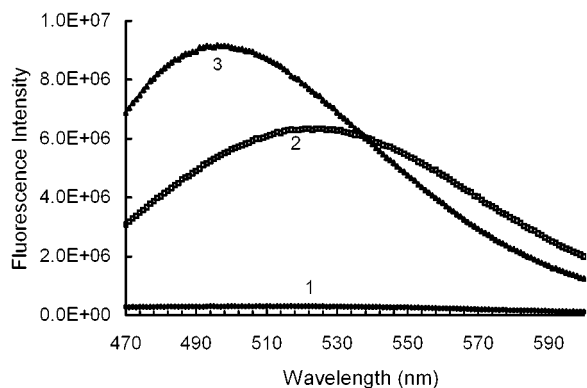
Figure 1. Fluorescence emission spectrum of FLSNO **9** in PBS buffer (curve 1), after transnitrosation with 50 molar equiv of GSH for 40 min (curve 2), and after irradiation at 365 nm for 50 min (curve 3). The initial concentration of **9** is 40 μM, and the excitation wavelength (λ_{ex}) is 323 nm.

and NO free radical (eq 2).[11] Figure 1 illustrates the fluorescence spectra of FLSNO **9** before and after the removal of the NO group (with both methods). The fluorescence enhancements of all FLSNOs as well as relevant data are summarized in Table 1.

The fluorescence enhancement values obtained from methods A and B overall demonstrate quite similar trends; that is, larger A_2/A_1 values correspond to larger B_2/B_1. With varied fluorophores (yet linked with roughly similar flexible alkyl linkers), the enhancements for FLSNOs **1**−**4** differ substantially. The fluorescence enhancements of both 6-aminoquionine-labeled **1** and 2-cyanoisoindole-labeled **3** were rather poor (close to unity), whereas 2-aminopyridine-labeled **2** and dansyl-labeled **4** showed relatively large enhancements. Given that the UV−vis absorption by primary or secondary aliphatic *S*-nitrosothiol consists of a 340 nm band (n → π^* transition) and a weaker 540 nm band (π → π^* transition), apparently the overlap between the absorption bands of

the SNO moiety and the fluorophore emission for **2** (361 nm) is better than that for either **1** (∼380 nm) or **3** (∼433 nm), whereas this overlap appears most efficient between the emission from dansyl (**4**) and SNO absorption at 540 nm. These observations are indeed consistent with the intramolecular energy transfer mechanism described by Forster's formalism (eq 3).[16]

$$k_T \propto \kappa^2 J R^{-6} \qquad (3)$$

where k_T is the rate of excited-state energy transfer from a donor to an acceptor, J is the overlap integral of donor emission and acceptor absorption, κ^2 is the relative spatial orientation of the transition dipoles of the donor and the acceptor, and R is the donor-to-acceptor distance. Here the k_T value is equivalent to the "net" fluorescence enhancement ($A_2/A_1 − 1$).[17]

The energy transfer rationale is further supported by the low fluorescence enhancement value for dansyl-labeled tertiary aliphatic *S*-nitrosothiols **5** and **6**. As recently suggested by Bartberger et al.,[18] tertiary alkyl substitution (R) prefers an anti conformation for the R−S−N=O moiety, thereby shifting the UV−vis absorption of the SNO moiety to around 590 nm. This would lead to poorer spectral overlap between dansyl fluorescence emission and SNO absorption, and therefore, little fluorescence enhancement is observed.

Because the energy transfer mechanism (eq 3) predicts large sensitivity of the fluorescence enhancement toward the donor-to-acceptor distance (R), we further examined dansyl-labeled compounds by varying the length of the alkyl linker (FLSNOs **7**−**12**). With a shorter linker (number of methylene units $n = 2$), FLSNO **7** exhibited little fluorescence enhancement. FLSNO **8**, similar to **4** in alkyl linker ($n = 3$), had a correspondingly strong enhancement. FLSNOs **9** and **12** ($n = 4$) showed even larger enhancements (up to 30-fold). As the length of linker was increased further in **10** ($n = 5$) and **11** ($n = 6$), however, the fluorescence enhancement *decreased* somewhat. From a simple consideration that the dansyl-to-SNO distance corresponds to the length of linker, the above results are quite unexpected and thus merit further investigation at the electronic structure level.

Theoretical Study of the Geometry and Energetics of SNO Interacting with Dansyl Ring. For an intramolecular energy transfer process, the donor-to-acceptor distance R strongly influences the k_T value (eq 3), and the distance, in turn, depends on the flexibility of the intramolecular donor-to-acceptor linkage. As a simplified treatment, we assume that only conformers with the closest donor-to-acceptor approach dominate the energy transfer process, provided that these conformers have reasonable populations (i.e., that they have energies close to the global minimum). To probe the conformational energy and the fluorophore-to-SNO distance with respect to the alkyl length, theoretical calculations were performed for the dansyl-labeled FLSNOs **7**−**12** using ab initio (HF/3-21G*) and density functional theory (B3LYP/6-31G**) calculations.

(16) Forster, Th. *Ann. Phys. (Berlin)* **1948**, *2*, 55.
(17) (a) Lakowicz, J. R. *Principles of Fluorescence Spectroscopy*; Plenum Press: New York, 1983; Chapter 10. (b) Cheung, H. C. In *Topics in Fluorescence Spectroscopy: Principles*; Lakowicz, J. R., Ed.; Plenum Press: New York, 1991; Vol. 2, pp 127−176.
(18) Bartberger, M. D.; Houk, K. N.; Powell, S. C.; Mannion, J. D.; Lo, K. Y.; Stamler, J. S.; Toone, E. J. *J. Am. Chem. Soc.* **2000**, *122*, 5889.

Table 1. Fluorescence Excitation and Emission Wavelengths (λ_{ex} and λ_{em}), Fluorescence Intensities,[a] and Fluorescence Enhancement Values[b] during Denitrosation of FLSNOs 1−12

FLSNO	λ_{ex} (nm)	λ_{em} (nm)	$10^{-5}A_1$	$10^{-5}A_2$	A_2/A_1	$10^{-5}B_1$	$10^{-5}B_2$	B_2/B_1
1	340	381	50	37	0.7	49	48	1.0
2	300	361	5.5	22	4.3	5.3	28	5.2
3	350	433	12	11	0.9	12	19	1.6
4	368	532	4.0	25	6.1	4.3	86	20
5	370	540	16	17	1.0	17	16	0.9
6	330	530	21	38	1.8	19	27	1.4
7	323	530	47	56	1.2	37	234	6.3
8	327	532	13	66	5.1	15	232	15
9	323	525	3.2	63	20	3.1	92	30
10	325	530	3.2	54	17	2.8	81	29
11	326	530	2.1	31	15	1.6	45	28
12	330	525	2.0	40	20	1.9	26	14

[a] Fluorescence intensities A_1 and A_2 are for transnitrosation between FLSNO and GSH (eq 1); B_1 and B_2 are for photolysis of FLSNO (eq 2), where the subscripts 1 and 2 refer to the fluorescence intensity of FLSNO before and after denitrosation, respectively. Slit: 0.25×0.25. [b] The estimated error bars for the ratio are $\pm15\%$ on the basis of repeated measurements.
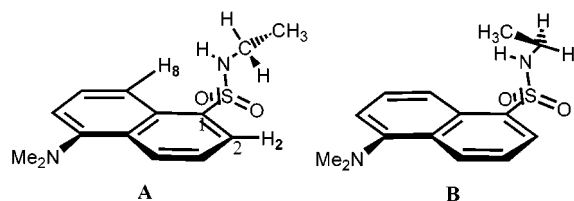
Figure 2. Nonoverlapping (**A**) and overlapping (**B**) conformations of dansyl ethane.

We first examined the geometries of the sulfonamide unit in the dansyl moiety, using unsubstituted 5-(dimethylamino)-1-naphthalenesulfonamide and its *N*-alkyl derivative as models (Figure 2). Optimization at the HF/3-21G* level revealed several features of the dansyl sulfonamide group (SO_2NH_2): (i) both N−H bonds of the sulfonamide nitrogen are eclipsed with the S=O bonds, and (ii) the rotation of the SO_2NH_2 group about the C−S bond is significantly constrained, with fairly high rotational barriers due to the steric repulsion between NH_2 and naphthalene hydrogens (∼11.6 kcal/mol for H_8 and 4.0 kcal/mol for H_2, respectively; see Supporting Information). This suggests that the dansyl sulfonamide unit is fairly rigid, with its S−N bond preferring an upright orientation (dihedral angle $\angle C_2-C_1-S-N$ is ∼112°). Calculations with *N*-methyl substitution suggested that an *N*-alkyl group would be tilted toward H_2, because the steric repulsion between *N*-alkyl and H_2 is around 1 kcal/mol smaller than that between *N*-alkyl and H_8. Next, we examined the conformations of *N*-ethyl substitution. As shown in Figure 2, the terminal methyl group can be oriented either away from the dansyl ring (conformer **A**) or toward the dansyl ring (conformer **B**). The energy of **A** is about 0.5 kcal/mol lower than that of **B**, suggesting that the steric repulsion between the dansyl ring and the alkyl chain would slightly favor a "nonoverlapping" conformation.

On the basis of the geometries of conformers **A** and **B** in Figure 2, a conformational search of dansyl-labeled FLSNOs was carried out by replacing a C−H bond of the *N*-alkyl substituent with the C−SNO moiety (Figure 3). For all the conformers, the SNO moiety adopts a syn orientation with its N=O bond eclipsing an αC−H bond,[18] while the alkyl chains (for $n \geq 4$) adopt essentially anti conformations to avoid gauche interactions. The nonoverlapping conformers (Figure 3A) were compared with the overlapping forms (Figure 3B) in terms of electronic energy ΔE and enthalpy ΔH, and the distance between the nitrogen in the SNO moiety and the center of the
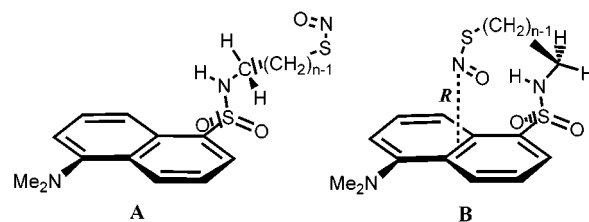

Figure 3. Nonoverlapping (**A**) and overlapping (**B**) conformations for FLSNOs **7−11**. For **B**, R is the closest dansyl-to-SNO distance.

Table 2. Computed Closest Dansyl-to-SNO Distance (R), Number of Methylene Units (n), and Corresponding Relative Energetic Preference (ΔE and ΔH) in Dansyl-Labeled FLSNOs (7−12) at 298 K

FLSNO	n	R^a	ΔE^b	ΔH^b
7	2	7.74	(0)	(0)
8	3	6.33	(0)	(0)
9	4	4.73^c	0.9	0.8
10	5	4.79	0.3	0.1
11	6	5.57	0.3	0.0
12	4^d	4.71^c	0.5	0.4

[a] Distance (Å) between the nitrogen in the SNO moiety and the center of the naphthalene ring (Figure 3B), calculated from the geometries optimized at the HF/3-21G* level. [b] Energy difference (ΔE and ΔH, in kcal/mol) between non-overlapping and overlapping conformations (Figure 3) calculated at the B3LYP/6-31G**//HF3-21G* level, $\Delta E = E - E_{ov}$. ΔH was obtained from ΔE and the difference in thermal corrections to enthalpy. [c] Averaged value of two conformers with nearly identical energies. [d] $(CH_2)_3C(CH_3)$ as the linker.

dansyl ring (R) was examined. The relevant results are summarized in Table 2.

For FLSNOs **7** and **8**, the SNO moiety is situated away from the dansyl ring in the most stable conformation ($\Delta E = 0$), and bringing the SNO group over the dansyl ring leads to an energy rise of around 1 kcal/mol (Figure 4). This is consistent with the results for *N*-ethyl substitution (Figure 2). As the length of the linker (n) increases, however, the SNO moiety in FLSNOs **9** and **12** ($n = 4$) prefers to approach the dansyl ring. These overlapping conformers are actually global minima (i.e., positive values for ΔE or ΔH). Apparently, in the overlapping conformations of **9** and **12**, the inherent steric repulsion between the alkyl chain and the dansyl ring is overcome by the attractive interaction between the SNO moiety and the dansyl ring.[19] Even longer alkyl linkers ($n = 5, 6$) lead to *weaker* preferences for the SNO−dansyl overlap, as indicated by smaller ΔE values for **10** and **11**. Consideration of solvent effects and entropy may alter
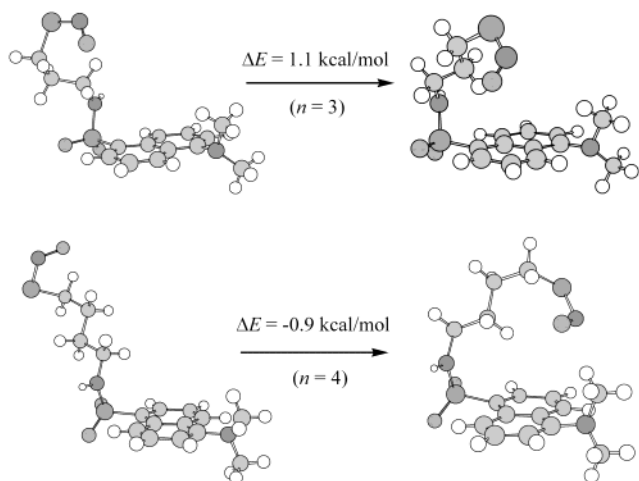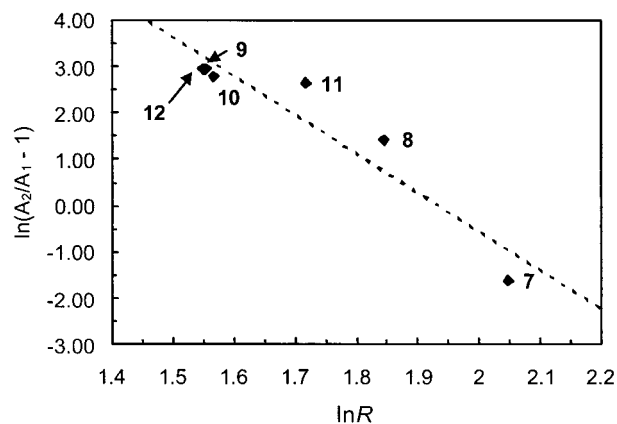
Figure 4. Conformational preference for FLSNOs **8** ($n = 3$) and **9** ($n = 4$) based on B3LYP/6-31G**//HF/3-21G* calculations.

the relative energies somewhat; nevertheless, the present calculations indicate that the overlapping conformers should play an important role in the intramolecular energy transfer in FLSNOs **9–12**.

The preceding survey of conformational preferences allows a meaningful comparison of the dansyl-to-SNO distances R in these structures (Table 2). It is interesting that the preference for an overlapping conformation (positive ΔE value) corresponds to a decrease in the R value, which also reaches a minimum for $n = 4$ ($\sim$4.7 Å for **9** and **12**). This suggests that the dansyl-to-SNO approach is indeed optimal at this linker length. The relatively rigid Ar–S(O)$_2$–NH unit is a contributing factor in determining the optimal length. The upright orientation of SO$_2$NH allows the alkyl chain on the sulfonamide nitrogen to be oriented either away from or toward the dansyl ring, with only a small energy increase for the latter (Figure 2). A short alkyl chain ($n = 2$) prevents the SNO moiety from reaching the dansyl ring primarily because of steric repulsion, leading to a significantly larger R value. In FLSNO **8**, three methylene units allows for closer dansyl-to-SNO approach ($R = 6.33$ Å) than that in **7** ($n = 2$). On the other hand, too long a linker ($n \geq 5$) with an anti orientation slightly increases the R values for **10** and **11**, which weakens the attractive interaction between the SNO moiety and the dansyl ring.[19] Clearly the length of the alkyl linker significantly influences the dansyl-to-SNO approach by switching the balance between steric repulsion and attractive interaction.

Moreover, for the most stable conformations of FLSNOs **7–12**, it is noted that a decrease in R corre-

Figure 5. Plot of the logarithm of "net" fluorescence enhancement [$\ln(A_2/A_1 - 1)$] versus the logarithm of the closet dansyl-to-SNO distance (ln R) in FLSNOs **7–12**.

sponds to an increase in fluorescence enhancement (Table 1). As shown in Figure 5, a roughly linear correlation can be found between the logarithm of R and the logarithm of "net" fluorescence enhancement ($A_2/A_1 - 1$).[20] This further supports the energy transfer rationale for the described fluorescence enhancement effect.
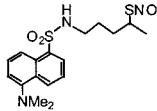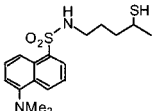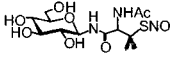
Kinetic Study of SNO/SH Transnitrosation with FLSNO and Its Parent Thiol. The exchange of nitroso group between *S*-nitrosothiol and thiol (eq 1) has been regarded as an intracellular pathway of NO transfer and also as a potential mechanism for the modification of protein activity.[21] It has been known that the SNO/SH transnitrosation is accomplished through nucleophilic attack of the nitroso nitrogen by the thiolate anion generated from thiol, and therefore, factors including the acidity of the sulfhydryl group, the pH of the reaction medium, and the stereoelectronic effects (e.g., charge, steric hindrance, inductive effect) of the substrates would come into play.[10,22] For example, it was reported that the nucleophilic attack on the nitroso nitrogen atom is favored by the electron-withdrawing substitution[10c] as well as by a positive charge close to the SNO moiety.[10i] Because the SNO/SH transnitrosation is rapid and reversible, most of the previous kinetic studies of NO transfer between different thiols have been based on monitoring the UV–visible absorption changes of RSNOs.[10a–f] Because of the low molar absorption coefficients of the *S*-nitroso chromophore ($\epsilon_{340} = 800$ M^{-1} cm^{-1} and $\epsilon = 20$ M^{-1} cm^{-1} around 540–600 nm), however, high concentrations of RSNOs are often required in these direct spectroscopic methods.

The large fluorescence enhancement after NO transfer from FLSNOs **9** and **12** to GSH demonstrates that fluorescence emission of these FLSNOs is far lower than that of the corresponding thiol (FL–SH), and this may

(19) (a) The interaction between the SNO moiety and the dansyl ring can be evaluated from the isodesmic reaction FL–SNO + CH$_3$-CH$_2$–H* → FL–H* + CH$_3$CH$_2$–SNO, where the geometry of the starred species is derived from the parent C–SNO compound (optimized at the HF/3-21G* level of theory); the C–SNO moiety is replaced by the C–H bond whose bond length is set at 1.08 Å, and other geometry parameters (bond angles and dihedral angles) are the same as those of the C–SNO moiety. The B3LYP/6-31G**//HF/3-21G* calculation showed that, for FLSNOs **7–12**, the stabilizing interactions are 0.3 (**7**), 0 (**8**), 1.0 (**9**), 0.5 (**10**), 0.5 (**11**), and 1.3 (**12**) kcal/mol, respectively. (b) Our recent experimental and theoretical study of the interaction between the aromatic amino acid side chain and *S*-nitrosothiols indicated that the binding energy between the aromatic ring and the SNO moiety is fairly sizable ($\sim$ 5 kcal/mol) and is probably electrostatic by nature. Vignini, A.; Akhter, S.; Wen, Z.; Schlegel, H. B.; Wang, P. G.; Mutus, B. Manuscript submitted for publication.

(20) It should be noted that Forster's equation (eq 3) describes a quantitative relationship between the energy transfer efficiency and the *average* value of donor-to-acceptor distance, where the relative spatial orientation of the transition dipoles of the donor and acceptor also plays a role. Because of the flexibility of the alkyl linker in FLSNOs **7–12** as well as the multiple polarizations for many chromophores, a constant value of κ^2 ($^2/_3$) is often adopted (Haas, E.; Katchalski-Katzir, E.; Steinberg, I. Z. *Biochemistry* **1978**, *17*, 5064.), and this allows direct correlation between $\ln(A_2/A_1 - 1)$ and $\ln(R)$.

(21) Stamler, J. S. *Curr. Top. Microbiol. Immunol.* **1995**, *196*, 19.

(22) (a) Butler, A. R.; Flitney, F. W.; Williams, D. L. H. *Trends Pharmacol. Sci.* **1995**, *16*, 18. (b) Huok, J.; Singh, R.; Whitesides, G. M. *Methods Enzymol.* **1987**, *143*, 129. (c) Whitesides, G. M.; Lilburn, J. E.; Szajewski, R. P. *J. Org. Chem.* **1977**, *42*, 332.

Table 3. Second-Order Rate Constants (k_2, M^{-1} s^{-1}) for the RSNO/R′SH Transnitrosation (Eq 1) Determined by Using FLSNO 12 and Its Parent Thiol[a]

Entry	RSNO	R'SH	k_2
1		GSH	3.36
2		*N*-acetyl-L-Cysteine	1.90
3		NAP	2.67
4		L-Penicillamine	2.63
5		*N*-Ac-EALFQCG	2.63
6		BSA	46.8
7	GSNO		1.15
8	SNAP		0.11
9	(Glu-1-SNAP)		2.21

[a] All reactions were carried out in PBS buffer (containing 20% MeOH, 1 mM EDTA, pH 7.4) at 25 °C.

be used for quantitative analysis of FL−SH. In the present study, FLSNO **12** was selected for the investigation of the kinetics of NO transfer between different thiols, including *N*-acetyl-L-cysteine, L-penicillamine, *N*-acetyl-L-penicillamine (NAP), GSH, heptapeptide *N*-acetyl-Glu-Ala-Leu-Phe-Gln-Cys-Gly (Ac-EALFQCG), and bovine serum albumin (BSA). The transnitrosation kinetics was also examined between the parent thiol of **12** and *S*-nitrosothiols of biological significance, including *S*-nitrosoglutathione (GSNO), *S*-nitroso-*N*-acetyl-L-penicillamine (SNAP), and Glu−1-SNAP. By monitoring the fluorescence change in the PBS buffer, the pseudo-first-order rate constants (k_{off}) were obtained in the presence of a large excess of RSNO or RSH. The second-order rate constants (k_2) were obtained by plotting the k_{off} values as a function of [RSNO]$_0$ or [RSH]$_0$. In all of the kinetics experiments, the concentration of FLSNO **12** or its parent thiol was around 40 μM. The results of this study are summarized in Table 3.

As shown in Table 3, the k_2 values between FLSNO **12** and low molecular weight thiols were small, ranging from 0.11 to 3.36 M^{-1} s^{-1}. The magnitude of these data is consistent with results obtained by other methods.[10] The rate constant for the cysteine sulfhydryl in *N*-acetyl heptapeptide was quite close to that for tripeptide GSH, indicating their similar polar and steric environments. The NO transfer from **12** to BSA showed the largest rate constant in all of our experiments, comparable with the reported value for *S*-nitrosocysteine to BSA (52 M^{-1} s^{-1}).[10i] This relatively high reactivity of BSA in *S*-nitrosation has been attributed to the fact that the free sulfhydryl (Cys-34) is located in a hydrophobic pocket of the amino terminal domain and is in close proximity to anionic charge.

Reaction kinetics of the transnitrosation between the parent thiol of **12** and RSNO showed that the k_2 values of GSNO and Glu−1-SNAP are around 20-fold larger than those of SNAP. This may be related to the difference in the electrostatic interaction between the environment of the SNO moiety and the attacking thiolate anion. At pH 7.4, both SNAP and GSNO are anionic because of the deprotonation of the carboxylic group. The anionic α-carboxylate group is close to the SNO moiety in SNAP, whereas in GSNO this carboxylate−SNO distance would
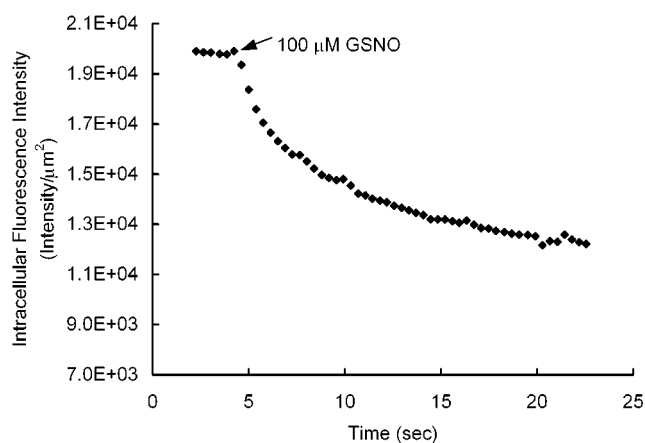
Figure 6. Quenching of intracellular fluorescence (λ_{ex} = 355 nm and λ_{em} = 515 nm, A = 0.501) in human umbilical vein endothelial cells (HUVECs, preincubated with FLSNO **12**) through introduction of extracellular GSNO (100 μM). The fluorescence intensity (intensity/μm^2) was calculated by Northern Eclipse Software 5.0. The results were averaged from quadruplicate studies.

be large because of semirigid carbamide units on both sides of the cysteine unit. The electrostatic repulsion between the carboxylate in SNAP and anionic thiolate (nucleophile) would, therefore, more strongly retard the nucleophilic attack than in GSNO. A similar mechanism may account for the much larger k_2 value for Glu−1-SNAP than for SNAP. Glu−1-SNAP is essentially neutral, and therefore, the attack of its nitroso nitrogen by thiolate would be easier than in SNAP despite their similar steric hindrance (two methyl groups).

Fluorescence Microscopic Study of FLSNO as a Probe for the Influx of RSNO-Bound NO through the Cellular Membrane. Because of its high reactivity, NO cannot exist in vivo mainly as a free radical. Instead, *S*-nitrosylated serum albumin and GSNO that are found in high concentrations in vivo may serve as NO carriers in the serum and in the cytosol.[23] The transfer of RSNO-bound NO conceivably should play a key role in physiological functions of NO. In this work, the large fluorescence enhancement for FLSNO **12** was used for probing the influx of NO in human umbilical vein endothelial cells (HUVECs). After HUVECs were loaded with FLSNO **12** and the extracellular FLSNO was removed, the digitized fluorescence images of the cells were obtained via a fluorescence microscope, and the fluorescence intensity of HUVECs was calculated and corrected for background. Upon the introduction of extracellular GSNO (100 μM), the changes in both the image and the intensity of intracellular fluorescence were monitored with respect to time (Figure 6).

As shown in Figure 6, HUVECs exhibit strong intracellular fluorescence after being loaded with FLSNO **12**, indicating the formation of fluorescent thiol via denitrosation of FLSNO **12**. As reported in our recent study, this intracellular fluorescence was due to the transnitrosation from FLSNO to intracellular thiols and, therefore, could be an index of intracellular thiol level.[13] On the other hand, this also suggests that the HUVEC membrane is

(23) (a) Marks, D. S.; Vita, J. D. F.; Kneaney, J. F., Jr.; Welch, G. N.; Loscalzo, J. *J. Clin. Invest.* **1995**, *96*, 2630. (b) Liu, Z.; Rudd, M. A.; Freedman, J. E.; Loscalzo, J. *J. Pharmacol. Exp. Ther.* **1998**, *284*, 526.

permeable by FLSNO **12**. Upon subsequent addition of extracellular GSNO, the fluorescence of HUVECs was rapidly quenched; the decrease in fluorescence intensity in the first 2 s accounts for about half of the total loss. This fluorescence quenching should be attributed to the NO transfer from extracellular GSNO to fluorescent dansyl-labeled thiol in the cytosol, where **12** is regenerated.

So far, the chemistry of NO transport through the cellular membrane has not yet been clarified. Previously, it was suggested that the NO free radical, owing to its charge neutrality and relatively low reactivity, diffuses freely across the cell membrane.[24] On the basis that the cell membrane contains a significant thiol pool,[25] it has recently been shown that the cellular entry of NO involves an SNO/SH transnitrosation that is catalyzed by cell surface protein disulfide isomerase (PDI).[26] The present result demonstrated that the reversible transnitrosation-induced change in fluorescence intensity between **12** and its parent thiol is a fairly sensitive probe of the intracellular GSNO-bound NO transfer, and thus, this type of FLSNO can be applied in further mechanistic studies of RSNO-bound NO transport through cellular membranes.

In summary, the present survey of twelve fluorophore-labeled *S*-nitrosothiols revealed that the largest increase in fluorescence intensity upon removal of the nitroso moiety was found for dansyl-linked *S*-nitrosothiols (FLSNOs **9** and **12**) where the linker (alkyl chain) contains four methylene units. The degree of fluorescence enhancement depends not only on the spectral overlap between the fluorophore emission and the SNO absorption but also on the structure of the linker. A theoretical study revealed that the dansyl-to-SNO approach in **9** and **12** is indeed energetically most preferred, whereby the stabilizing interaction between the SNO moiety and dansyl ring compensates for the steric repulsion better than with either longer or shorter linkers.

Using dansyl-linked FLSNO **12**, the kinetic study of SNO/SH transnitrosation suggested that a carboxylate group that is in close proximity to a nitroso nitrogen disfavors the nucleophilic attack in transnitrosation. The fluorescence microscopic study showed that the reversible change in fluorescence intensity for **12** could be a sensitive probe for intracellular RSNO-bound NO transport.

Experimental Section

Synthesis of Fluorophore-Labeled *S*-Nitrosothiols (FLSNO 1−12). All chemicals were obtained from commercial suppliers and used without further purification. All NMR spectra were recorded on a Varian Unity-500, Varian Unity-400 MHz (^{1}H), or Mercury 400 MHz spectrometer. NMR chemical shifts were expressed in ppm relative to internal solvent peaks, and coupling constants were measured in Hz. MS spectra were obtained from a Kratos 80 MS spectrometer (ionization mode: EI, ESI, or FAB). UV−visible spectroscopy measurements were carried out on a HP 8453 UV−visible spectrometer (Hewlett-Packard Co.).

FLSNO 1. To a solution of 6-aminoquinoline (436 mg, 3 mmol) in anhydrous DMF (20 mL) was added NaH (115 mg, 3.0 mmol, 60%) at 0 °C under argon. The brown mixture was

(24) Goretski, J.; Hollocher, T. *J. Biol. Chem.* **1988**, *263*, 2316.

(25) (a) Ammon, H.; Hagele, R.; Youssif, N.; Eujen, R.; El-Amri, N. *Endocrinology* **1983**, *112*, 720−726. (b) Redelman, D.; Hudig, D. *Adv. Exp. Med. Biol.* **1985**, *184*, 527.

(26) Zai, A.; Rudd, A.; Scribner, A. W.; Loscalzo, J. *J. Clin. Invest.* **1999**, *103*, 393.

stirred for 30 min, followed by the addition of *N*-acetyl homocysteine thiolactone (481 mg, 3 mmol) in DMF (15 mL). The solution was warmed to room temperature, stirred for another 5 h, and quenched with water. The aqueous phase was extracted with CHCl$_3$ (50 mL × 3), and the combined organic solution was dried over anhydrous Na$_2$SO$_4$, concentrated, and purified via flash chromatography (5% MeOH in CHCl$_3$) to give thiol **13** (545 mg, 60%). ^{1}H NMR (300 MHz, CDCl$_3$): δ 9.89 (s, 1H), 8.48 (d, *J* = 1.5 Hz, 1H), 8.12 (d, *J* = 1.5 Hz, 1H), 7.79 (d, *J* = 9.0 Hz, 1H), 7.66 (d, *J* = 9.0 Hz, 1H), 7.43−7.59 (m, 1H), 7.07 (m, 1H), 4.48−4.60 (m, 1H), 2.25−2.38 (m, 2H), 1.80−1.95 (m, 2H), 1.75 (s, 3H). ^{13}C NMR (75 MHz, CD$_3$OD): δ 170.8, 170.7, 149.0, 145.2, 136.6, 135.8, 129.6, 128.7, 123.7, 121.5, 115.9, 52.7, 36.8, 23.0, 21.0. HRMS calcd for C$_{15}$H$_{17}$O$_2$N$_3$S, 303.1041; found, 303.1042.

To a solution of **13** (150 mg, 0.5 mmol) in MeOH (5 mL) was added *tert*-butyl nitrite (1.5 mL) dropwise over 5 min with stirring at −20 °C in the dark. The solution was stirred at −20 °C for 2 h and concentrated at room temperature in the dark to give **1** as a red oil. ^{1}H NMR (400 MHz, CD$_3$OD): δ 8.77 (dd, *J* = 4.5, 1.6 Hz, 1H), 8.38 (d, *J* = 2.4 Hz, 1H), 8.36 (d, *J* = 8.7 Hz, 1H), 7.96 (d, *J* = 9.0 Hz, 1H), 7.86 (dd, *J* = 9.0, 2.4 Hz, 1H), 5.40 (dd, *J* = 8.1, 4.5 Hz, 1H), 4.69 (dd, *J* = 9.0, 5.6 Hz, 1H), 2.54−2.68 (m, 2H), 2.07−2.20 (m, 2H), 2.05 (s, 3H). ^{13}C NMR (100 MHz, CD$_3$OD): δ 172.5, 171.6, 148.0, 143.2, 138.3, 137.4, 129.2, 127.3, 124.9, 121.8, 116.4, 53.4, 36.4, 21.3, 20.3. EIMS: 333 (M$^+$ + 1).

FLSNO 2. This compound was prepared from 2-aminopyridine and *N*-acetyl homocysteine thiolactone in a manner similar to that described previously. ^{1}H NMR (400 MHz, CD$_3$-OD): δ 8.21−8.31 (m, 1H), 7.81−8.05 (m, 2H), 7.15−7.30 (m, 1H), 4.67 (dd, *J* = 8.8, 4.8 Hz, 1H), 2.54−2.68 (m, 2H), 2.03 (s, 3H), 1.99−2.19 (m, 2H). ^{13}C NMR (100 MHz, CD$_3$OD): δ 172.7, 172.3, 150.6, 145.0, 141.0, 120.3, 115.1, 53.4, 35.9, 21.2, 20.3.

FLSNO 3. 1,2-Phthalic dicarboxaldehyde (132 mg, 1 mmol), homocysteine thiolactone hydrochloride (155 mg, 1 mmol), and NaCN (54 mg, 1.1 mmol) were dissolved in MeOH (5 mL) and water (5 mL). The mixture was stirred in the dark for 4 h, followed by the addition of water. The aqueous phase was extracted with CH$_2$Cl$_2$. The organic phase was dried over anhydrous Na$_2$SO$_4$. After the removal of solvent, the residue was purified by silica gel column chromatography (hexanes/EtOAc, 8:2) to give **14** (118 mg, 50%). ^{1}H NMR (400 MHz, CDCl$_3$): δ 7.65 (d, *J* = 8.0 Hz, 1H), 7.60 (d, *J* = 8.8 Hz, 1H), 7.33 (s, 1H), 7.24−7.28 (m, 1H), 7.11 (dd, *J* = 8.8, 6.4 Hz, 1H), 5.33 (dd, *J* = 13.2, 7.4 Hz, 1H), 3.59−3.52 (m, 1H), 3.48−3.42 (m, 1H), 3.06−2.99 (m, 1H), 2.77−2.66 (m, 1H). ^{13}C NMR (100 MHz, CDCl$_3$): δ 200.3, 131.7, 126.3, 124.8, 123.6, 121.0, 118.4, 118.3, 117.7, 114.1, 67.4, 33.1, 27.4.

To a solution of **14** (100 mg, 0.40 mmol) in MeOH (10 mL) was added NaBH$_4$ (40 mg, 1.2 mmol) in one portion at 0 °C. The mixture was stirred for 3.5 h and was quenched with water. The aqueous solution was extracted with EtOAc. The extract was dried over anhydrous Na$_2$SO$_4$ and concentrated to give the crude product. Purification was through a silica gel column (hexanes/EtOAc, 5:5) to give the thiol (67 mg, 65%). ^{1}H NMR (400 MHz, CDCl$_3$): δ 7.64 (d, *J* = 8.0 Hz, 1H), 7.62 (d, *J* = 7.6 Hz, 1H), 7.48 (s, 1H), 7.26−7.23 (m, 1H), 7.11 (dd, *J* = 8.4, 6.8 Hz, 1H), 4.85−4.80 (m, 1H), 4.04 (dd, *J* = 11.6, 6.4 Hz, 1H), 3.95 (d, *J* = 11.6 Hz, 1H), 2.50−2.28 (m, 4H). ^{13}C NMR (100 MHz, CDCl$_3$): δ 131.8, 125.9, 124.6, 123.2, 121.0, 118.2, 118.0, 114.9, 65.1, 61.4, 35.6, 20.9. To a solution of the thiol (51 mg, 0.20 mmol) in MeOH (1.5 mL) and water (0.5 mL) was added HNO$_2$ (1.20 mL, 1.0 M) dropwise over 5 min at −20 °C in the dark. In the dark, the mixture was stirred for another 2 h and concentrated at room temperature. The residue was extracted with absolute anhydrous ethanol (1 mL). The filtrate was evaporated in the dark to give pure FLSNO **3** in 78% yield. ^{1}H NMR (400 MHz, CDCl$_3$): δ 7.47 (m, 2H), 7.51 (s, 1H), 7.26 (dd, 1H, *J* = 8.0, 7.2 Hz), 7.13 (dd, *J* = 8.0, 7.2 Hz, 1H), 4.56−4.60 (m, 1H), 4.02 (dd, *J* = 11.6, 6.0 Hz, 1H), 3.94 (dd, *J* = 11.6, 4.4 Hz, 1H), 3.30−3.46 (m, 2H), 2.36−2.47 (m, 2H). ^{13}C NMR (100 MHz, CDCl$_3$): δ 131.8, 126.1, 124.7, 123.4, 121.1, 118.3, 117.9, 114.7, 65.0, 61.9, 31.3, 29.3.

FLSNO 4. This compound was prepared from dansyl chloride and homocysteine thiolactone in a manner similar to that described previously. ^{1}H NMR (400 MHz, CD$_3$OD): δ 8.94 (d, J = 8.8 Hz, 1H), 8.70 (d, J = 8.8 Hz, 1H), 8.43 (d, J = 7.6 Hz, 1H), 8.11 (d, J = 7.2 Hz, 1H), 7.85–7.92 (m, 2H), 3.48 (s, 6H), 3.27–3.40 (m, 3H), 3.05–3.31 (m, 2H), 1.41–1.75 (m, 2H). ^{13}C NMR (100 MHz, CD$_3$OD): δ 139.5, 138.0, 130.6, 129.5, 127.7, 127.5, 127.0, 126.1, 125.8, 119.5, 64.3, 54.8, 46.8, 30.3, 29.6.

FLSNO 5. This compound was prepared from dansyl chloride and *S*-trityl penicillamine methyl ester. ^{1}H NMR (400 MHz, CD$_3$OD): δ 8.53–8.57 (m, 2H), 8.24 (d, J = 6.4 Hz, 1H), 7.62–7.68 (m, 2H), 7.61 (d, J = 7.6 Hz, 1H), 3.76 (s, 1H), 3.01 (s, 6H), 2.97 (s, 3H), 1.32 (s, 3H), 1.29 (s, 3H). ^{13}C NMR (100 MHz, CD$_3$OD): δ 169.7, 135.7, 130.1, 129.7, 129.3, 127.9, 123.9, 121.4, 116.1, 66.0, 50.7, 45.1, 44.7, 29.4, 27.6. EIMS: 426 (M$^+$ + 1).

FLSNO 6. The mixture of 3,3-dimethyl acrylaldehyde (21.8 g), benzyl mercaptan (35 mL), and piperidine (1.5 mL) was heated by steam bath for 6.5 h. The Michael addition product was purified by distillation under reduced pressure. The aldehyde (31.6 g, 60%) was collected at the bp 109–110 °C/15 mmHg. ^{1}H NMR (CDCl$_3$, 300 MHz): δ 9.82 (t, J = 2.7 Hz, 1H), 7.23–7.35 (m, 5H), 3.79 (s, 2H), 2.545 (d, J = 3.0 Hz, 2H), 1.46 (s, 6H). To a stirred slurry of NaBH$_4$ (3.05 g) in ethyl ether (200 mL) at 0 °C was added the above aldehyde (26.2 g) in methanol (15 mL) dropwise over 2 h. The reaction mixture was stirred at 0 °C for another 2 h, followed by the evaporation of solvent, and the residue was dissolved in water. The aqueous solution was extracted with Et$_2$O (100 mL $\times$ 3), and the combined ether solution was dried over anhydrous Na$_2$SO$_4$. After the removal of solvent, the residue was purified by distillation to give alcohol **15** (19.0 g, bp 135–137 °C/1.5 mmHg, 72%). ^{1}H NMR (300 MHz, CDCl$_3$): δ 7.22–7.35 (m, 5H), 3.82 (dt, J = 6.6 Hz, 5.7 Hz, 2H), 3.77 (s, 2H), 2.40 (t, J = 5.7 Hz), 1.85 (t, J = 6.6 Hz), 1.36 (s, 6H). HRMS calcd for C$_{12}$H$_{18}$OS, 210.1078; found, 210.1082.

To a solution of **15** (6.05 g, 30 mmol) in anhydrous THF (20 mL) at −78 °C under nitrogen was added BuLi (19.0 mL, 1.6 M in hexane). The reaction mixture was stirred for another 0.5 h, followed by the addition of toluenesulfonyl chloride (5.75 g, 30 mmol) in THF (30 mL) in one portion, and warmed to room temperature. After 0.5 h the solvent was removed at −78 °C. The residue was purified via flash chromatography (hexanes/EtOAc, 9:1) to give the tosylate as an oil (9.57 g, 95%). ^{1}H NMR (300 MHz, CDCl$_3$): δ 7.79 (d, J = 7.8 Hz, 2H), 7.34 (d, J = 7.8 Hz, 2H), 7.21–7.28 (m, 5H), 4.20 (t, J = 7.2 Hz, 2H), 3.62 (s, 2H), 2.44 (s, 3H), 1.92 (t, J = 7.2 Hz, 2H), 1.28 (s, 6H). A mixture of the above tosylate (11.6 g, 32.7 mmol) and NaCN (2.450 g, 50 mmol) in DMF (60 mL) was stirred at 70 °C overnight. The solution was cooled to room temperature and diluted with water (200 mL). The aqueous solution was extracted with Et$_2$O (100 mL $\times$ 3), and the combined organic phase was dried over anhydrous Na$_2$SO$_4$. Removal of solvent gave the crude product, which was purified with silica gel column chromatography (hexane/EtOAc 20:1) to give **16** (6.25 g, 90%) as a pale yellow oil. ^{1}H NMR (300 MHz, CDCl$_3$): δ 7.25–7.33 (m, 5H), 3.69 (s, 2H), 2.44 (t, J = 7.8 Hz, 2H), 1.83 (t, J = 7.8 Hz, 2H), 1.33 (s, 6H). ^{13}C NMR (75 MHz): δ 138.1, 129.1, 128.9, 127.4, 120.3, 45.7, 37.5, 33.3, 28.8, 13.3. HRMS calcd for C$_{13}$H$_{17}$NS, 219.1082; found, 219.1083.

To a solution of LiAlH$_4$ (1.15 g, 30 mmol) in THF was added the solution of **16** (6.25 g, 28.4 mmol) in THF (40 mL) at 0 °C in 30 min. The mixture was refluxed for 6 h, cooled to 0 °C, and quenched by water (1 mL), 15% NaOH (1.5 mL), and water (5 mL). The mixture was filtered, and the solid residue was washed three times with hot THF. The combined organic solution was dried over anhydrous Na$_2$SO$_4$ and concentrated. The crude product was purified via flash chromatography (hexanes/EtOAc 4:1) to give the amine (3.32 g, 55%). ^{1}H NMR (300 MHz, CDCl$_3$): δ 7.17–7.33 (m, 5H), 3.68 (s, 2H), 2.57–2.62 (m, 2H), 1.49–1.52 (m, 4H), 1.28 (s, 6H), 1.20 (br s, 2H). ^{13}C NMR (75 MHz, CDCl$_3$): δ 138.8, 129.2, 128.6, 127.0, 46.3, 42.8, 39.8, 33.2, 29.3, 29.1. HRMS calcd for C$_{13}$H$_{21}$NS, 223.1395; found, 223.1394. To anhydrous ammonia (60 mL) in a three-

necked round flask at −40 °C was added the above amine (2.236 g, 10 mmol), followed by the addition of sodium metal (1.25 g) in several portions to keep the reaction mixture blue. Water (2 mL) was added to quench the reaction after 1.5 h, and the mixture was allowed to warm to room temperature, while nitrogen was bubbled to evaporate ammonia gas. The residue was dissolved in water. The aqueous solution was extracted with CHCl$_3$ (30 mL $\times$ 3), and the combined organic phase was dried over Na$_2$SO$_4$. After the removal of solvent, the crude product was purified with silica gel column chromatography (CH$_2$Cl$_2$/MeOH 10:1) to give **17** as a colorless oil (0.904 g, 70%). ^{1}H NMR (300 MHz, CDCl$_3$): δ 2.64 (br s, 2H), 1.66 (br s, 3H), 11.44 (m, 4H), 1.29 (s, 6H). ^{13}C NMR (75 MHz, CDCl$_3$): δ 44.7, 43.9, 42.5, 33.0, 29.6. EIMS: 103 (M$^+$, 50), 89 (36), 74 (72), 67 (35), 59 (33).

To a solution of **17** (200 mg, 1.5 mmol) and 4-(dimethylamino)pyridine (365 mg, 3 mmol) in anhydrous CH$_2$Cl$_2$ (10 mL) was added a solution of dansyl chloride (375 mg, 1.4 mmol) in CH$_2$Cl$_2$ (10 mL) dropwise over 20 min at 0 °C. The mixture was stirred for another 30 min from 0 °C to room temperature. After the removal of the solvent, the residue was purified via flash chromatography (hexanes/EtOAc 8:2) to give thiol **18** as a green oil (370 mg, 71%). ^{1}H NMR (300 MHz, CDCl$_3$): δ 8.51 (d, J = 8.4 Hz, 1H), 8.34 (d, J = 8.4 Hz, 1H), 8.24 (dd, J = 7.5, 1.2 Hz, 1H), 7.46–7.55 (m, 2H), 7.15 (d, J = 7.2 Hz, 1H), 5.31 (t, J = 6.3 Hz, 1H), 2.92 (td, J = 6.6, 6.3 Hz, 2H), 2.85 (s, 6H), 1.37–1.45 (m, 2H), 1.23–1.32 (m, 2H), 1.1 (s, 6H). ^{13}C NMR (75 MHz, CDCl$_3$): δ 152.2, 135.2, 130.6, 130.1, 129.9, 129.8, 128.6, 123.4, 119.2, 115.5, 45.7, 44.2, 43.7, 43.4, 32.6, 25.7. ESIMS: 771 ((2M + K)$^+$), 755 ((2M + Na)$^+$), 405 ((M + K)$^+$), 389 ((M + Na)$^+$).

Following procedures described previously, FLSNO **6** was prepared from **18** (92%). ^{1}H NMR (400 MHz, CD$_3$OD): δ 8.89 (d, 1H, J = 8.8 Hz), 8.75 (d, J = 8.8 Hz, 1H), 8.32 (d, J = 7.2 Hz, 1H), 8.19 (d, J = 8.0 Hz, 1H), 7.82–7.88 (m, 2H), 3.54 (s, 6H), 2.94 (t, J = 6.4 Hz, 2H), 1.90 (td, J = 8.0, 4.0 Hz, 2H), 1.64 (s, 6H), 1.39–1.44 (m, 2H). ^{13}C NMR (100 MHz, CD$_3$OD): δ 139.2, 137.9, 130.1, 129.4, 127.7, 127.6, 127.0, 126.0, 125.8, 119.8, 56.1, 46.9, 42.9, 40.1, 27.9, 25.0. ESIMS: 813 ((2M + Na)$^+$), 791 ((2M + H)$^+$), 434 ((M + K)$^+$), 418 ((M + Na)$^+$), 396 ((M + H)$^+$).

Typical Procedure for the Synthesis of Dansyl-Labeled *S*-Nitrosothiols (FLSNO 9). To a solution of 4-amino-1-butanol (100 mg, 1.1 mmol) and Et$_3$N (0.35 mL) in anhydrous CH$_2$Cl$_2$ (15 mL) was added dansyl chloride (270 mg, 1 mmol) in CH$_2$Cl$_2$ (10 mL) dropwise over 10 min. The solution was stirred at room temperature for another 2 h. After the removal of solvent, the residue was purified by silica gel column chromatography (hexanes/EtOAc 8:2) to give pure **19** (264 mg, 83%). ^{1}H NMR (300 MHz, CDCl$_3$): δ 8.55 (d, J = 8.7 Hz, 1H), 8.30 (d, J = 8.7 Hz, 1H), 8.24 (dd, J = 7.5, 1.2 Hz, 1H), 7.50–7.58 (m, 2H), 7.19 (d, J = 7.2 Hz, 1H), 5.20 (t, J = 6.0 Hz, 1H), 3.51 (m, 2H), 2.91–2.93 (m, 2H), 2.90 (s, 3H), 1.46–1.54 (m, 4H).

A solution of **19** (325 mg, 1.0 mmol) and Et$_3$N (1.5 mL) in anhydrous CH$_2$Cl$_2$ (25 mL) was cooled to −20 °C under nitrogen atmosphere and stirred for 30 min, followed by the addition of toluenesulfonyl chloride (195 mg, 1 mmol) in one portion. The solution was kept in the refrigerator overnight. After the removal of solvent, the crude product was purified via flash chromatography (hexanes/EtOAc 8:2) to give the tosylate as a viscous oil (431 mg, 92%). ^{1}H NMR (300 MHz, CDCl$_3$): δ 8.51 (d, J = 8.4 Hz, 1H), 8.27 (d, J = 8.4 Hz, 1H), 8.18 (d, J = 7.5 Hz, 1H), 7.68 (d, J = 7.8 Hz, 2H), 7.45–7.52 (m, 2H), 7.27 (d, J = 7.8 Hz, 2H), 7.14 (d, J = 7.8 Hz, 1H), 5.31 (t, J = 6.3 Hz, 1H), 3.82 (t, J = 5.7 Hz, 2H), 2.85 (s, 6H), 2.80 (m, 2H), 2.38 (s, 3H), 1.47–1.56 (m, 2H), 1.34–1.43 (m, 2H). ^{13}C NMR (75 MHz, CDCl$_3$): δ 152.2, 145.1, 134.9, 132.9, 130.7, 130.2, 130.0, 129.7, 129.6, 128.7, 128.0, 123.4, 118.9, 115.5, 70.1, 45.6, 42.6, 25.9, 25.8, 21.9. A solution of the tosylate (256 mg, 0.55 mmol) and potassium thioacetate (250 mg, 2.2 mmol) in acetone (10 mL) was stirred at room temperature for 4 h, followed by evaporation of solvent. The residue was purified with silica gel column chromatography to give **20** with quantitative yield. ^{1}H NMR (300 MHz,

CDCl$_3$): δ 8.47 (d, J = 8.7 Hz, 1H), 8.31 (d, J = 8.7 Hz, 1H), 8.19 (d, J = 7.5 Hz, 1H), 7.42−7.49 (m, 2H), 7.10 (d, J = 7.5 Hz, 1H), 5.61 (t, J = 6.3 Hz, 2H), 2.84−2.87 (m, 2H), 2.80 (s, 6H), 2.58 (t, J = 6.3 Hz, 2H), 2.20 (s, 3H), 1.33−1.39 (m, 4H). ^{13}C NMR (75 MHz, CDCl$_3$): δ 196.2, 152.1, 135.2, 130.5, 130.0, 129.8, 129.6, 128.6, 123.4, 119.2, 115.4, 45.6, 42.8, 30.8, 28.7, 28.49, 26.61.

To a solution of **20** (195 mg, 0.51 mmol) in anhydrous CH$_2$-Cl$_2$ (10 mL) at −78 °C under argon atmosphere was added DIBALH (2.2 mL, 1 M in hexanes) dropwise over 10 min. The solution was stirred at −78 °C for another 2 h and quenched with cold, diluted hydrochloric acid. The aqueous phase was extracted with Et$_2$O, and the combined organic solution was dried over anhydrous Na$_2$SO$_4$ and concentrated. The crude product was purified via flash chromatography (hexane/EtOAc 8:2) to give thiol **21** in 70% yield. ^{1}H NMR (300 MHz, CDCl$_3$): δ 8.53 (d, J = 8.7 Hz, 1H), 8.30 (d, J = 9.0 Hz, 1H), 8.23 (dd, J = 7.5 Hz, 1.2 Hz, 1H), 7.48−7.56 (m, 2H), 7.16 (d, J = 6.9 Hz, 1H), 5.28 (t, J = 6.3 Hz, 1H), 2.87−2.92 (m, 2H), 2.87 (s, 6H), 2.23−2.30 (m, 2H), 1.40−1.45 (m, 4H). ^{13}C NMR (75 MHz, CDCl$_3$): δ 152.2, 135.0, 130.7, 130.1, 129.8, 129.7, 128.7, 123.4, 119.0, 115.5, 45.7, 42.9, 30.9, 28.4, 24.2. HRMS calcd for C$_{16}$H$_{22}$O$_2$N$_2$S$_2$, 338.1123; found, 338.1126.

To a solution of thiol **21** (121 mg, 0.35 mmol) in MeOH (1.5 mL) and water (0.5 mL) at −20 °C in the dark was added HNO$_2$ (1.30 mL, 1.0 M) dropwise over 5 min. The mixture was stirred for another 2 h, followed by evaporation at room temperature in the dark. The residue was extracted with absolute anhydrous ethanol (1 mL). The filtrate was evaporated in the dark to give pure **9** in 85% yield. ^{1}H NMR (400 MHz, CD$_3$OD): δ 8.88 (d, J = 8.8 Hz, 1H), 8.67 (d, J = 8.8 Hz, 1H), 8.35 (d, J = 6.4 Hz, 1H), 8.16 (d, J = 8.4 Hz, 1H), 7.83−7.91 (m, 2H), 3.53 (s, 6H), 3.35−3.54 (m, 2H), 2.89 (t, J = 6.6 Hz, 2H), 1.28−1.42 (m, 4H). ^{13}C NMR (100 MHz, CD$_3$OD): δ 139.3, 137.9, 130.1, 129.4, 127.5, 127.4, 126.9, 126.0, 125.6, 119.6, 46.7, 42.1, 37.6, 28.4, 25.9. ESIMS: 368 (M$^+$ + 1).

FLSNO 7. This compound was prepared in a manner similar to that described above. ^{1}H NMR (300 MHz, CD$_3$OD): δ 8.88 (d, J = 8.4 Hz, 1H), 8.67 (d, J = 8.7 Hz, 1H), 8.33 (d, J = 7.2 Hz, 1H), 7.84−7.93 (m, 2H), 3.52 (s, 6H), 3.45−3.25 (m, 2H), 3.05 (t, J = 6.6 Hz, 2H). ^{13}C NMR (75 MHz, CD$_3$OD): δ 139.4, 137.4, 130.2, 129.5, 127.6, 127.4, 126.9, 125.8, 119.6, 46.7, 41.5, 37.1. ESIMS: 378 (M$^+$ + K), 362 (M$^+$ + Na), 340 (M$^+$ + 1).

FLSNO 8. This compound was prepared in a manner similar to that described above. ^{1}H NMR (300 MHz, CD$_3$OD): δ 8.92 (d, J = 8.7 Hz, 1H), 8.64 (d, J = 8.7 Hz, 1H), 8.36 (d, J = 7.5 Hz, 1H), 8.15 (d, J = 7.5 Hz, 1H), 7.86−7.93 (m, 2H), 3.51 (s, 6H), 3.25−3.55 (m, 2H), 2.87 (t, J = 6.9 Hz, 2H), 1.54−1.64 (m, 2H). ^{13}C NMR (75 MHz, CD$_3$OD): δ 139.4, 137.5, 130.2, 129.4, 127.6, 127.4, 126.9, 126.1, 125.7, 119.6, 46.7, 41.5, 34.7, 28.9. ESIMS: 392 (M$^+$ + K), 376 (M$^+$ + Na), 354 (M$^+$ + 1).

FLSNO 10. This compound was prepared in a manner similar to that described above. ^{1}H NMR (300 MHz, CD$_3$OD): δ 8.92 (d, J = 8.4 Hz, 1H), 8.64 (d, J = 9.0 Hz, 1H), 8.55 (dd, J = 7.6, 1.2 Hz, 1H), 8.16 (d, J = 7.6 Hz, 1H), 7.85−7.91 (m, 2H), 3.51 (s, 6H), 3.30−3.45 (m, 2H), 2.86 (t, J = 6.6 Hz, 2H), 1.29−1.36 (m, 4H), 1.10−1.28 (m, 2H). ^{13}C NMR (75 MHz, CD$_3$-OD): δ 139.5, 137.8, 130.0, 129.5, 127.5, 127.4, 126.9, 126.1, 125.5, 119.5, 46.7, 42.4, 38.0, 28.3, 28.2, 25.4. EIMS: 382 (M$^+$ + 1).

FLSNO 11. This compound was prepared in a manner similar to that described above. ^{1}H NMR (300 MHz, CD$_3$OD): δ 8.93 (d, J = 9.0 Hz, 1H), 8.76 (d, J = 8.7 Hz, 1H), 8.35 (d, J = 7.2 Hz, 1H), 8.21 (d, J = 7.8 Hz, 1H), 7.85−7.92 (m, 2H), 3.54 (s, 6H), 3.35−3.45 (m, 2H), 2.84 (t, J = 7.0 Hz, 2H), 1.27−1.38 (m, 2H), 1.07−1.17 (m, 2H). ^{13}C NMR (75 MHz, CD$_3$OD): δ 139.0, 137.8, 130.1, 129.5, 127.7, 127.6, 127.0, 125.9, 125.7, 119.8, 46.8, 42.6, 32.7, 29.2, 28.6, 27.9, 25.7.

FLSNO 12. To a solution of **19** (350 mg, 1.1 mmol) in anhydrous CH$_2$Cl$_2$ (20 mL) was added pyridinium dichromate (1.6 equiv) in several portions over 3 h at 0 °C until the substrate disappeared. The mixture was filtered through a short Celite column, and the filtrate was concentrated. The crude product was dissolved in anhydrous THF (10 mL). To this solution was added MeLi solution (1.0 M in hexane, 4 mL, 4.0 mmol) dropwise at −78 °C under nitrogen. The solution was stirred for another 2.5 h at −78 °C and quenched by MeOH. After workup, the crude product was purified by silica gel chromatography to give **22** as a green oil (207 mg, 60%, two steps). ^{1}H NMR (300 MHz, CDCl$_3$): δ 8.49 (d, J = 8.7 Hz, 1H), 8.32 (d, J = 8.4 Hz, 1H), 8.20 (dd, J = 7.2, 1.2 Hz, 1H), 7.50−7.44 (m, 2H), 7.12 (d, J = 8.1 Hz, 1H), 5.87 (t, J = 7.6 Hz, 1H), 3.58−3.52 (m, 1H), 2.89−2.81 (m, 2H), 2.83 (s, 6H), 2.49 (br s, 1H), 1.46−1.39 (m, 2H), 1.28−1.20 (m, 2H), 0.95 (d, J = 6.0 Hz, 3H). ^{13}C NMR (75 MHz, CDCl$_3$): δ 152.0, 135.1, 130.5, 130.0, 129.8, 129.6, 128.6, 123.4, 119.2, 115.4, 67.6, 45.6, 43.4, 40.0, 36.0, 23.6.

FLSNO **12** can be obtained from alcohol **22** by following the procedure for the synthesis of **9**. ^{1}H NMR (300 MHz, CD$_3$OD): δ 8.90 (d, J = 9.3 Hz, 1H), 8.78 (d, J = 8.7 Hz, 1H), 8.34 (d, J = 6.6 Hz, 1H), 8.22 (d, J = 7.6 Hz, 1H), 7.84−7.92 (m, 2H), 4.05−4.15 (m, 1H), 3.56 (s, 1H), 2.87 (t, J = 6.3 Hz, 2H), 1.20−1.28 (m, 2H), 1.33−1.51 (m, 2H), 1.156 (d, J = 7.2 Hz, 3H). ^{13}C NMR (75 MHz, CD$_3$OD): δ 139.1, 137.8, 130.2, 129.4, 127.7, 127.6, 127.0, 126.0, 125.8, 119.9, 46.8, 42.2, 32.4, 26.9, 19.2. ESIMS: 785 ((2M + Na)$^+$), 763 ((2M + H)$^+$), 421 ((M + K)$^+$), 404 ((M + Na)$^+$), 382 ((M + 1)$^+$).

General Procedure for Evaluating the Fluorescence Enhancement of Synthetic Fluorophore-Labeled *S*-Nitrosothiols. The fluorescence spectra were recorded with a SPEX FluoroMax spectrometer. All reactions were carried out in PBS buffer (1.0 mM EDTA, 20% MeOH). In the experiment of transnitrosation with free thiols (method A), the fluorescence emission spectrum of the substrate (40 μM) in the buffer was measured to record the emission intensity (A_1), then excess GSH (50 equiv) was added, and the fluorescence emission was monitored over time, from which the maximum intensity (after around 40 min) was recorded (A_2) to derive fluorescence enhancement ratio (A_2/A_1). Photolytic denitrosation (method B) was performed as follows: the solution of FLSNO was exposed to UV (365 nm) irradiation, during which the time-dependent fluorescence intensity was recorded. The maximum emission intensity (B_2) was compared with the intensity of fluorescence emission recorded before irradiation (B_1) to derive the fluorescence enhancement ratio (B_2/B_1).

General Procedure for the Kinetic Study of Transnitrosation Using FLSNO 12. All materials were purified before use. Following the literature procedure, *S*-nitroso-*N*-acetylpenicillamine (SNAP),[27] Glu−1-SNAP,[14a] and *N*-Ac-EALFQCG[28] were synthesized. Preparation of GSNO is described in the next section. All reactions were carried out in PBS buffer (containing 20% methanol and 1 mM EDTA, pH 7.4). The fluorescence emission spectra (λ_{ex} = 330 nm, λ_{em} = 540 nm) were obtained using a SPEX FluoroMax spectrometer. First, it was confirmed that the fluorescence intensity of the parent thiol of **12** responds linearly to the concentration of thiol in the presence of excess GSH (Supporting Information). The pseudo-first-order rate constant k_0 was determined by reacting FLSNO **12** with a ~15−35-fold amount of thiol or by reacting the thiol of **12** with a ~15−35-fold amount of *S*-nitrosothiol. All reactions were carried out at 25 °C, and the initial concentration of **12** or its thiol was 40 μM. During the reaction, the fluorescence intensity of the mixture was measured at 525 nm every 2 min. Very good first-order behavior was generally found in this study. The second-order rate constant k_2 for each reaction was obtained by plotting k_0 as a function of [RSNO]$_0$ or [RSH]$_0$.

Fluorescence Microscopic Study of Intracellular Fluorescence Quenching with the Use of FLSNO 12. (A) Preparation of GSNO. To a solution of GSH in ice cold 0.5 M HCl was added equimolar sodium nitrite in the dark at 4 °C over 40 min. The pH of the reaction was adjusted to 7.0,

(27) Field, L.; Dilts, R.; Ravichandran, R.; Lenhert, P. G.; Carnahan, G. E. *J. Chem. Soc., Chem. Commun.* **1978**, 249.

(28) Xian, M.; Wang, Q. M.; Chen, X.; Wang, K.; Wang, P. G. *Bioorg. Med. Chem. Lett.* **2000**, *10*, 2097.

and the product GSNO was crystallized by the slow addition of cold acetone.

(B) Cell Culture. Human umbilical vein endothelial cells (HUVEC-CRL 1730) were grown in Gibco's Ham F12K with L-glutamine (2 mM), sodium carbonate (1.5 g/L), heparin (100 μg/mL), endothelial cell growth supplement (50 μg), and fetal bovine serum (10%). The HUVECs were grown to confluence on slides (Erie Scientific) at 37 °C with atmospheric CO_2 (10%).

(C) Fluorescence Microscopy. HUVECs were loaded with FLSNO **12** ($A = 0.501$) for 2 min. Following a 4×30 s wash, GSNO (100 μM) was introduced. Fluorescence quenching images were obtained every 300 ms via a Zeiss Axiovert 35 microscope. The fluorescence intensity (intensity/μm^2) was calculated and corrected for background by a data acquisition system (Northern Eclipse 5.0).

Theoretical Calculations. All calculations were performed using the Gaussian 98 program package.[29] A conformational search was carried out for each molecule by full optimization at the HF/3-21G* level as mentioned in the text. A frequency

analysis was performed to verify the nature of each structure and to obtain zero-point energies (ZPEs) and thermal corrections to enthalpy. For conformations within 2 kcal/mol of the most stable structure, electron correlation effects were incorporated by single-point calculations at the B3LYP/6-31G** level to identify the minimum energy conformation in the gas phase. The structures, electronic energies, and thermal corrections to enthalpies of all compounds (FLSNO **7**−**12**) are provided in the Supporting Information.

Supporting Information Available: ^{1}H, ^{13}C NMR spectra for FLSNOs **1**−**12**; mass spectra for FLSNOs **1**, **5**−**10**, and **12**; plot of fluorescence intensity versus the concentration of parent thiol of FLSNO **12** in the presence of excess GSH; plots of the time course of fluorescence intensity in the transnitrosation between **12** and GSH as well as between GSNO and the parent thiol of **12**; plot of the pseudo-first-order rates versus the initial concentrations of GSH in the transnitrosation between **12** and GSH; relaxed potential energy surface for the rotation of the SO_2NH_2 group around the C−S bond in 5-(dimethylamino)-1-naphthalenesulfonamide (HF/3-21G*); HF/3-21G* optimized structures, total electronic energies computed at the B3LYP/6-31G** level and thermal corrections to enthalpy for FLSNOs **7**−**12**. This material is available free of charge via the Internet at http://pubs.acs.org.

JO015658P

(29) Frisch, M. J.; Trucks, G. W.; Schlegel, H. B.; Scuseria, G. E.; Robb, M. A.; Cheeseman, J. R.; Zakrzewski, V. G.; Montgomery, J. A., Jr.; Stratmann, R. E.; Burant, J. C.; Dapprich, S.; Millam, J. M.; Daniels, A. D.; Kudin, K. N.; Strain, M. C.; Farkas, O.; Tomasi, J.; Barone, V.; Cossi, M.; Cammi, R.; Mennucci, B.; Pomelli, C.; Adamo, C.; Clifford, S.; Ochterski, J.; Petersson, G. A.; Ayala, P. Y.; Cui, Q.; Morokuma, K.; Malick, D. K.; Rabuck, A. D.; Raghavachari, K.; Foresman, J. B.; Cioslowski, J.; Ortiz, J. V.; Baboul, A. G.; Stefanov, B. B.; Liu, G.; Liashenko, A.; Piskorz, P.; Komaromi, I.; Gomperts, R.; Martin, R. L.; Fox, D. J.; Keith, T.; Al-Laham, M. A.; Peng, C. Y.; Nanayakkara, A.; Challacombe, M.; Gill, P. M. W.; Johnson, B.; Chen, W.; Wong, M. W.; Andres, J. L.; Gonzalez, C.; Head-Gordon, M.; Replogle, E. S.; Pople, J. A. *Gaussian 98*, rev. A.9; Gaussian, Inc.: Pittsburgh, PA, 1998.